



ORIGINAL ARTICLE

Effect of multipass friction stir processing and reinforcement particles on aluminum alloys of AA7010

Rohit Kumar, Rakesh Rajpal, Rajesh Kumar

Department of Manufacturing and Automation, School of Engineering and Technology, Soldha, Bahadurgarh, India

Article Information

Received: 09 June 2022
Revised: 14 July 2022
Accepted: 21 July 2022
Available online: 29 July 2022

Keywords:

Tensile strength;
Micro hardness;
Multipass FSP
Reinforcement particles

Abstract

The consequence of multipass FSP (MPFSP) and Reinforcement Particles SiC on mechanical characteristics FSPed region of AA7010 was successfully fabricated. The microstructure of MPFSP/SiC of AA7010 in the SZ was observed to be fine and equiaxed in the fifth pass FSP and found excellent mechanical properties compared to the base metal, and other FSP passes due to homogenously dispersed reinforced particles in the AMC. Reduced grain size and scattered SiC particles increased mechanical properties. In the 5th pass FSP, the reinforced particles are uniformly distributed and fragmented completely. The accumulation of reinforcement particles reduces as the FSP pass increases. AA7010 had a UTS of 348.31 MPa and a percent strain of 15.32. Tensile characteristics were improved as the FSP pass increased after using MPFSP with SiC nanoparticles on the AA7010. The maximum UTS measured after one, three, and five passes were 415.09 MPa, 438.72 Mpa, and 452.07 MPa, respectively. The VMHN at the stir zone were 119.2 HV, 126 HV, and 129.8 HV was perceived in the single pass, third pass and fifth pass FSP.

©2022 ijrei.com. All rights reserved

1. Introduction

Due to the numerous applications for aluminium alloys, their utilization has grown. This covers various structural applications, such as food packaging, aerospace, maritime shipbuilding, and car body building [1-3]. Aluminum alloys are used because of their attractive properties, such as their high strength-to-weight ratio, appearance, increased ductility, and simplicity of manufacture [4–7]. The alloying components used to create each alloy impact the mechanical and thermal characteristics of the various aluminium alloys [6-7]. However, it is common knowledge that material advancements are crucial for enhancing material performance and extending the lifespan of components [8]. Friction stir processing is one

of the numerous methods for improving materials' properties. Nano-sized ceramic particles like TiB₂, SiCp [9-11], Al₂O₃ [12], and ZrB₂ [13] have been added to alloy matrices to fabricate nano-particulate-reinforced alloy matrix composites to enhance the mechanical characteristics of aluminium alloys. It has been observed that the tensile ductility of such particle-reinforced alloys may be maintained or even improved with a concurrent rise in tensile strength, depending on the processing method, mainly by lowering the reinforcing particle size to the nanometer range [14-16]. But casting often reduces ductility and toughness because of flaws like porosity, particle-matrix bonding, and notably particle clustering [17, 18]. Agglomerates in the melt are pushed by the solidification front and eventually cluster along grain boundaries in solidification

Corresponding author: Rohit Kumar

Email Address: rohit33478@gmail.com

<https://doi.org/10.36037/IJREI.2022.6406>

[19, 20], making it impossible for even the most vigorous stirring procedures, such as ultrasonic dispersion during casting, to break them up. The 7XXX family of aerospace aluminium alloys are high-strength materials typically heat treated to offer the ideal blend of strength, toughness, and stress corrosion cracking resistance. They are precipitation-strengthened alloys, with the Mg₂Zn phase [21] serving as the primary strengthening precipitate. The heat treatment of the base metal creates a supersaturated solid solution in almost all precipitation hardening aluminium alloys: a solution heat treatment is followed by a quick quenching. The solid solution decomposes during an ageing process that entails one or more phases of keeping the material at a temperature lower than the solution treatment temperature. The microstructure that results from this dispersion of tiny precipitates is tuned. Depending on the type of welding and the particular parameters (heat input, welding speed) utilized, the temperature histories associated with any welding operation will affect the "optimal" microstructure to variable degrees. The existence of low-melting phases in many alloys from the 7XXX family, along with the fact that many precipitation hardening alloys include more alloying elements than can be brought into solid solution, can cause the occurrence of local melting at temperatures much below the bulk solidus. Significant microstructural refinement, densification, uniformity of the processed zone, and the removal of manufacturing process flaws have all been demonstrated to be achievable with FSP [22-24]. The mechanical characteristics of processed surfaces, such as hardness, tensile strength, fatigue, corrosion resistance, and wear resistance, have improved [25, 26]. The impact of process factors on the microstructure was assessed following a single pass in most FSP experiments. However, the microstructure of Al castings may be modified further with numerous FSP passes. To analyze the effects of multi-pass friction stir processed joints of aluminum alloys, identify a knowledge gap, and summarize the literature that is currently accessible on multi-pass FSP of aluminum alloys. In this work, the effect of multipass FSP (MPFSP) and reinforcement particles SiC on mechanical properties and microstructure was investigated.

2. Materials and Method

The base metal AA7010 was employed to fabricate the MPFSP/SiC. Plates were cut into the dimensions of 6.2 x 80 x 180 mm by an EDM machine. The groove was created on the center of the base plate with a dimension of 2.5 x 3 x 170 mm. This groove was filled by SiC reinforcement particles closed this groove with a pin-less tool with an RTS of 900 rev/min and a WS of 65 mm·min⁻¹. The process parameters of the MPFSP/SiC are shown in Table 1. During the MPFSP, a fixture was employed to avoid the misalignment of the fabricated plates demonstrated in Fig. 1. The FSP passes were varied from one to five, while the axial force (6.5 KN), tilt angle (2°), WS, and RTS were kept constant for all the specimens. The temperature peak of the MPFSP samples varied between 434 to 462°C, which was measured by an infrared thermometer. The square FSP tool made of H13 tool steel was used to

process the base plates. The tool's dimensions included a tool shoulder diameter of 19.5 mm, a tool pin length of 5.5 mm, and a 6 mm tool pin diameter. After the MPFSP, the emery papers were used to polish the processed region and etched all samples for about 10 s by Keller's reagent (82 ml H₂O, 8 ml HNO₃, 6 ml HCL, 4 ml HF) [27]. The tensile specimens were cut along the welding direction and perpendicular to the welding direction as per ASTM E8 standard [28]. The microstructure of MPFSP and fractured samples was examined by the scanning electron microscopy (SEM) machine and optical microscopy machine. A Vickers hardness machine studied the micro hardness test with a load of 100 g for 10 s as per the ASTM E384 standard.

Table 1: Processing parameter of friction stir processing

TRS (rpm)	TS (mm/min)	Nano SiC (%)	No of Pass
900	65	9	5
		6	5
		12	5
		9	3
		6	1
		12	1
		12	3
		9	1
		6	3

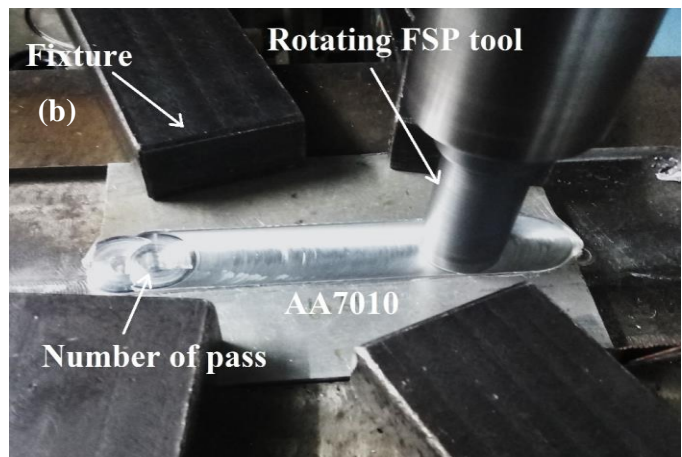
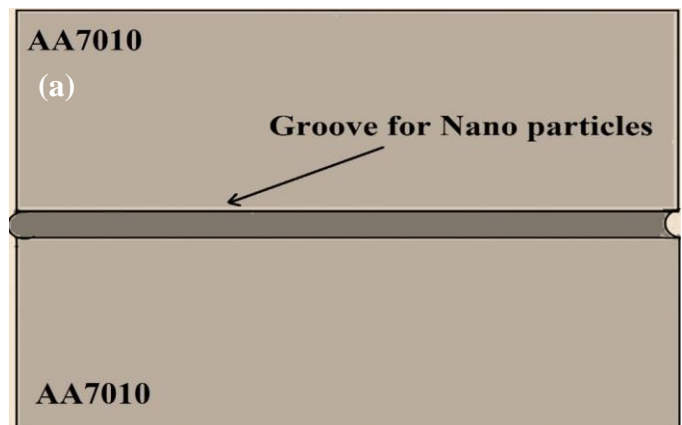


Figure 1: (a) Groove for reinforcement particles, (b) multipass FSP process

3. Results and Discussion

3.1 Ultimate Tensile Strength (UTS)

The influence of process parameters on the mechanical properties and microstructure of MPFSP with SiC nanoparticles has been evaluated. A UTM was employed to test three tensile samples for each MPFSP/SiC parameter as per the ASTM E8 standard. The true stress strain curve of MPFSP/SiC of Al-7010 of different parameters was demonstrated in fig. 2. As long as no reinforcing particles were utilized, the mechanical properties of FSP samples were primarily controlled by grain size. According to fig. 3, the fifth pass FSP'ed nanocomposite had the maximum tensile stress and elongation compared to other specimens. The improved tensile characteristics of MPFSP can be attributed to their more uniform reinforcement dispersion, fine grain size, and less clustered particles. Moreover, the bigger agglomerates and particle clusters in single-pass FSP nanocomposite may behave as preferred sites for fracture initiation [29]. Fig. 2 depicts the AMC stress-strain diagram after MPFSP/SiC of AA7010. The tensile strength of MPFSP/SiC increased from 350 MPa to 455 Pa as the FSP passes increased from 1 to 5. Because of the coarse grain structure and low hardness, the tensile specimens cracked in either the TMAZ or HAZ area. Previous studies have also reported fracture sites in HAZ and TMAZ [30, 31]. The UTS of the MPFSP/SiC of AA7010 was perceived to be higher than base metal due to grain refining and the equiaxed grain structure. The ductility and strength of defect-free MPFSP/SiC are influenced by the thermal characteristics of AA7010. The toughness of the MPFSP enhanced as the FSP pass increased. These findings may enhance the percentage of fragmentation and dispersion of reinforcement particles. It resists dislocation movement under axial loading. The MPFSP convinces SiC with Al-7010 composites of severe DRX, dispersion, fragmentation, and structural plasticization.

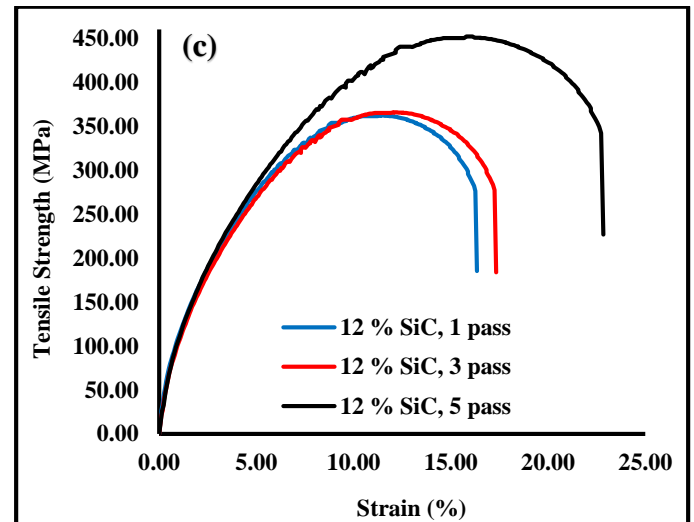
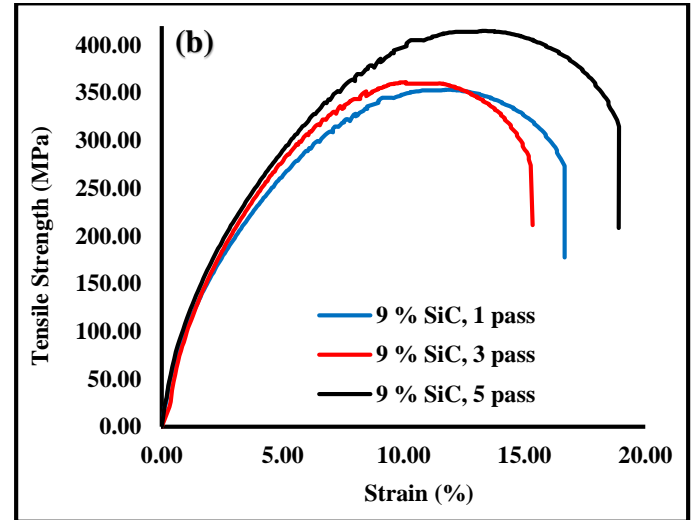


Figure 2: Stress-strain curve of Al-7010/SiC subjected to MPFSP, (a) 6% SiC, (b) 9% SiC, (c) 12% SiC

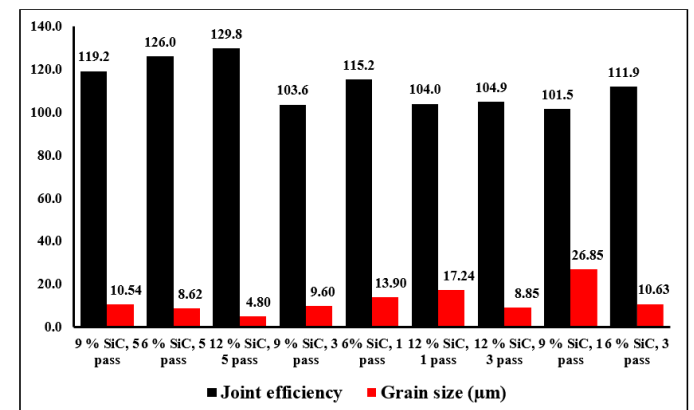
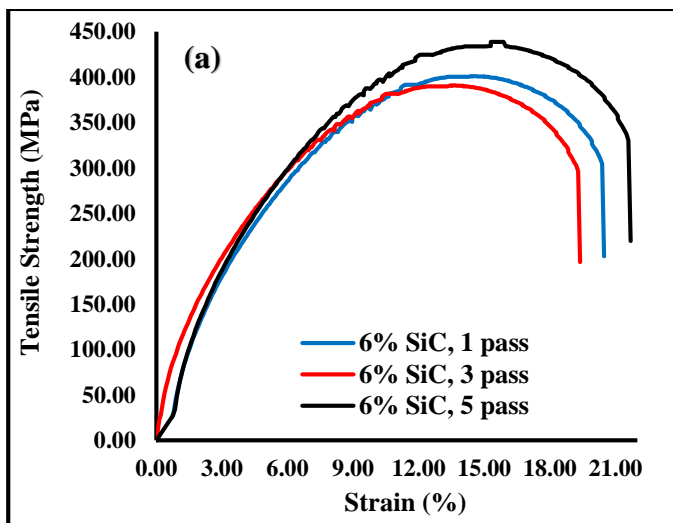


Figure 3: Variation of grain size and joint efficiency of MPFSP with SiC reinforcement particles.

Tensile characteristics were improved as the FSP pass increased after using MPFSP with SiC nanoparticles on the AA7010. As shown in fig. 3 and table 2, the maximum joint

efficiency and maximum UTS were 129.8% and 452.07 MPa was observed at rotational tool speed of 900 rpm, welding speed of 65 mm-min⁻¹ with 12% of reinforcement particles with 5th FSP pass.

3.2 Micro-Hardness

Fig. 4a-c depicts Vicker micro hardness number (VMHN) variation and distance from the weld center of MPFSP/SiC composite. As the FSP pass increases, so do the VMHN. Meanwhile, it could be related to the refinement and fragmentation of reinforcement particles. The presence of hard Nano (SiC), fragmented particles, and the fined grain structure

in the composite were related to the heat input of MPFSP. The maximum hardness value was observed as per the hall-Petch relationship [32, 33]. In the 5th pass FSP with 6, 9, and 12% SiC nanoparticles, the three most significant VMHN at the SZ were 126, 119.2, and 129.8 HV. The parent metal AA7010 had a mean indentation hardness of 96 HV, which increased to 129.8 HV in the fifth pass of FSP with the incorporation of a reinforcing agent of SiC reinforcement particles. The presence of hard reinforcement particles, increased dislocation density, and, most crucially, the fine grain size was the primary reason for enhancing the VMHN of multipass FSPed joints. Moreover, the 5th pass FSP sample has superior reinforcing particle distribution, resulting in minor variance in VMHN.

Table 2: Mechanical Properties of MPFSPed joints of AA7010

TRS (rpm)	TS (mm/min)	Nano SiC (%)	Number of FSP Pass	UTS	Strain (%)	Hardness (HV)	Joint efficiency (%)
900	65	9	5	415.09	19.84	118	119.2
		6	5	438.72	21.69	122	126.0
		12	5	452.07	22.84	125	129.8
		9	3	360.91	15.36	107	103.6
		6	1	401.16	20.48	112	115.2
		12	1	362.10	16.32	103	104.0
		12	3	365.50	17.3	109	104.9
		9	1	353.42	16.67	107	101.5
		6	3	389.63	19.36	113	111.9

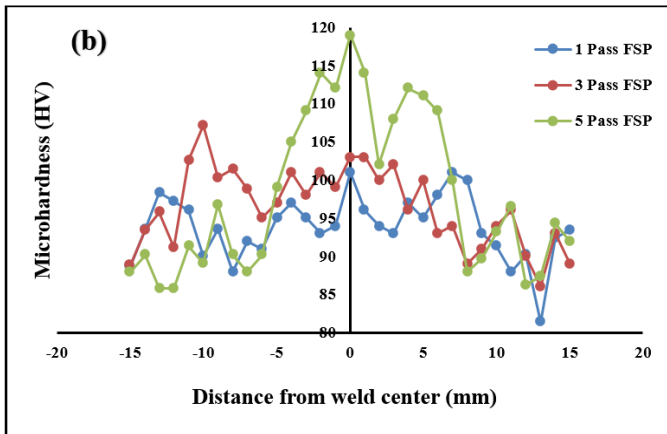
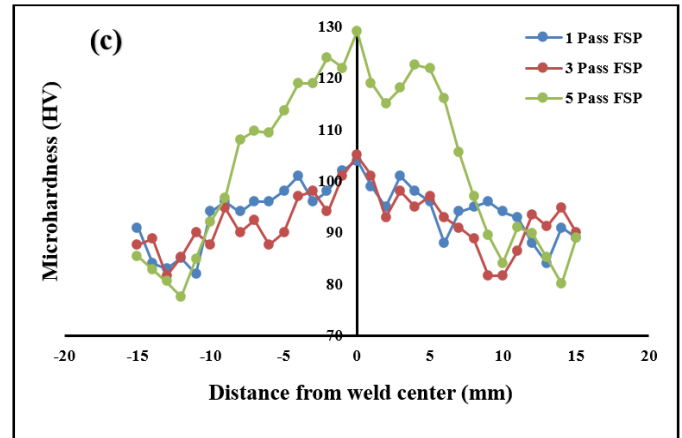
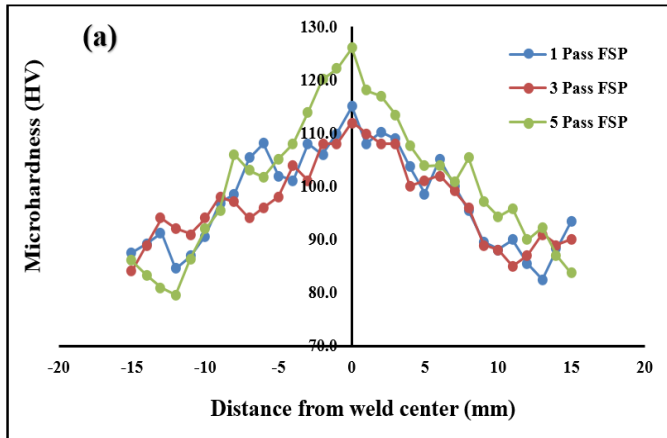


Figure 4: Variation of microhardness of MPFSP/SiC of AA7010, (a) 6% SiC, (b) 9% SiC, (c) 12% SiC

The microhardness value rose in MPFSP with filler SiC due to higher dislocation density and grain refining. During MPFSP, the heat and plastic strain was created by the DRX, while forming refined grain structure cause mechanical breakage of the intrinsic grain boundary. The reinforcement particles distributed in the parent material (AA7010) were accountable for grains boundary during MPFSP. The fragmentation of nanoparticles during MPFSP allows grains boundary to migrate [34]. A favorable location for additional refined and equiaxed grains were observed after DRX in MPFSP [35]. Five-pass FSP/SiC revealed an excellent grain structure as compared to other processed region. Thus, microhardness augmentation during MPFSP/SiC can be attributed to grain refining, and dispersion strengthening [36].

3.3 Microstructure Analysis

The optical microstructure of multipass FSP/SiC of AA7010, single pass, third pass and fifth pass FSP is shown in Fig. 6. The microstructure samples were polished using emery sheets (grade size 400 to 2000), and the disc polishing machine is used for final polishing with alumina powder. Following polishing, specimens were submerged into ASTM E407 killer reagent (82 ml H₂O, 5 ml hydrochloric acid, 4 ml hydrofluoric acid, and 8 ml Nitric acid). The equal distribution of refined grains in the SZ resulted from the appropriate softening of the metal, revealing the highest VMHN and UTS of the MPFSP [37]. The optical microstructure of the parent metal AA7010 was depicted in Fig.6a, and coarse grain size of $65 \pm 15 \mu\text{m}$ were perceived; the microstructure of AA7010 was significantly refined in the regions SZ in MPFSP. Image J software was used to assess the grain size of the MPFSP specimens, and the grains size of one pass, three passes, and five passes were determined to be $17.24 \mu\text{m}$, $8.85 \mu\text{m}$, $4.80 \mu\text{m}$, respectively for 12% SiC, as shown in fig. 5. The modified grain structure refinement of AA7010 towards SZ, TMAZ, and HAZ was gradually adjusted in one pass FSP. As shown in the figure, nanoparticles of SiC were added to improve the SZ

during the first, third, and fifth passes of FSP.

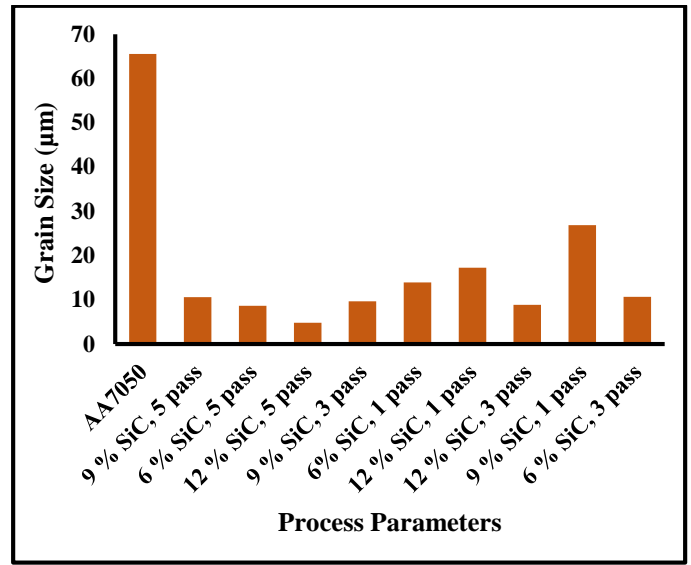


Figure 5: Comparison of grain size to the processing parameters of MPFSP/SiC of AA7010

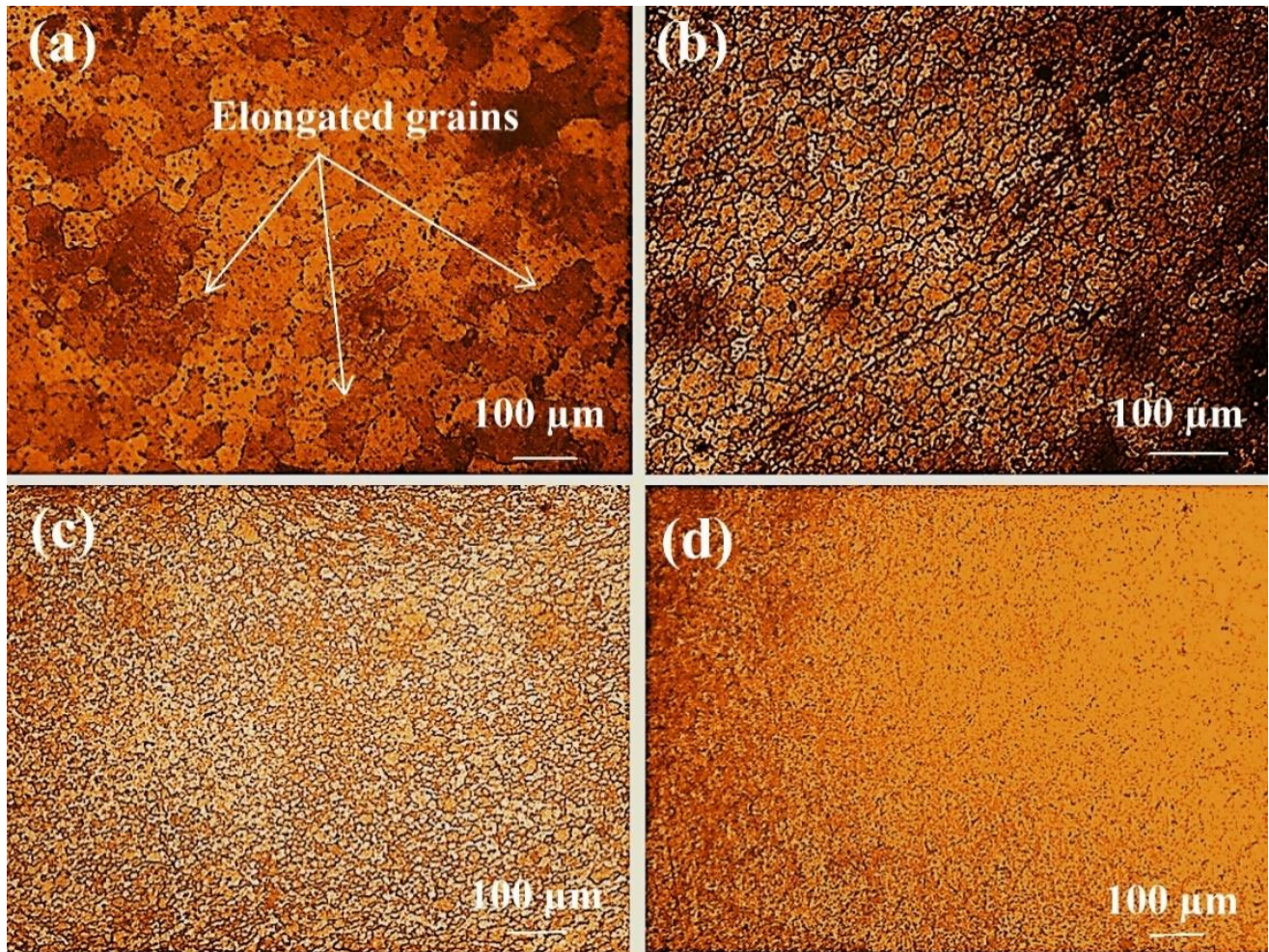


Figure 6: Optical microstructure of MPFSP/SiC, (a) Base metal A7010, (b) 1 pass, (c) 3 pass, (d) 5 pass

3.4 Fracture Analysis

The fracture analysis of multi-pass FSP/SiC was done by SEM machine and observed the failure pattern, tiny and ductile dimples on the multi-pass FSP samples. The higher area of tiny and ductile dimples and least amount of cleavage facets was observed in the five pass FSP/SiC. Fig. 7a-b depicts the fracture surfaces of the composite AA7010/SiC with one pass and five pass FSP. The shear plane of 45° to the tensile axis was formed along the periphery of the specimens during the tensile test, forming a cup-cone fracture [38]. The tiny and equiaxed dimples were observed in five pass FSP/SiC fractured sample which indicating ductile failure. One pass FSP/SiC specimen showed the honey comb dimples which shows microporous and agglomerative ductile fractures. The microstructure of the composite AA7010/SiC with fifth passes showed uniform and finer than the other passes, and it was also reveals from the fracture morphology that the dimple size in multi-pass FSP/SiC was smaller than the parent metal AA7010; that's why the mechanical properties of multi-pass FSP/SiC was much higher than the base metal AA7010.

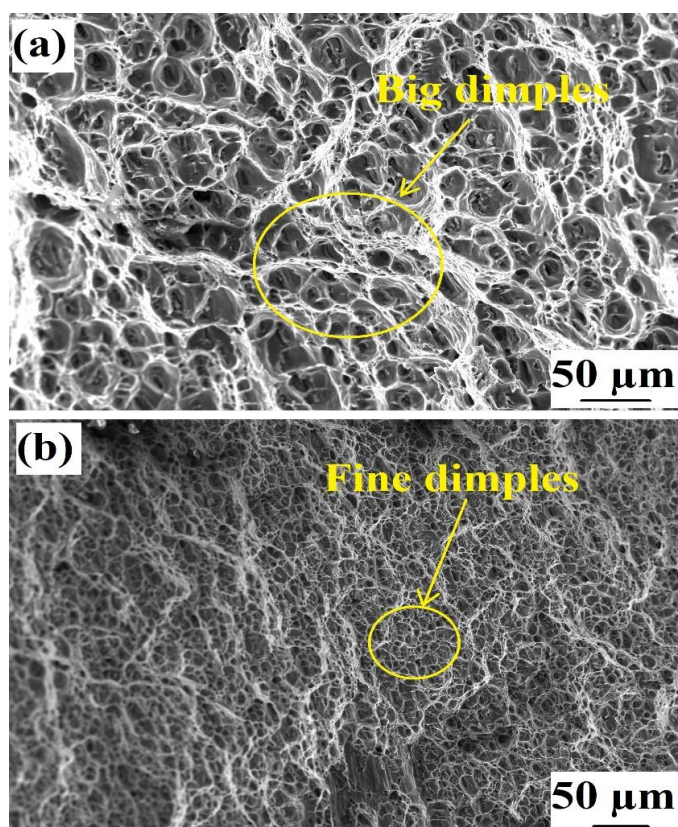


Figure 7: Fractography of AA7010/SiC composite, (a) one pass, (b) five passes

The ductile fracture with honeycomb dimples were observed in one pass FSP/SiC, and the separated features on the fracture surface showed characteristics of both plastic deformation and cleavage [39].

All multi-pass FSP samples processed at a constant TRS and

TS. During the multi-pass FSP/SiC, the uniform dispersion of reinforcement particles, consequently decreasing the grain size, effectual material mixing, fine and equiaxed dimples, were observed. All the multi-pass FSP/SiC samples were fractured in the HAZ or TMAZ region due to coarse grains structure and material softening as confirmed by variation in the microhardness.

4. Conclusions

The consequence of MPFSP and Reinforcement Particles SiC on mechanical characteristics FSPed region of AA7010 was successfully fabricated and found the following conclusions.

- The microstructure of MPFSP/SiC of AA7010 in the SZ was observed to be fine and equiaxed in the fifth pass FSP and found excellent mechanical properties compared to the base metal and other FSP passes due to homogeneously dispersed reinforced particles in the AMC.
- Reduced grain size and scattered SiC particles increased mechanical properties. In the 5th pass FSP, the reinforced particles are uniformly distributed and fragmented completely. The accumulation of reinforcement particles reduces as the FSP pass increases.
- AA7010 had a UTS of 348.31 MPa and a percent strain of 15.32. Tensile characteristics were improved as the FSP pass increased after using MPFSP with SiC nanoparticles on the AA7010. The maximum UTS measured after one, three, and five passes was 415.09 MPa, 438.72 MPa, and 452.07 MPa respectively.
- The VMHN at the stir zone were 119.2 HV, 126 HV, and 129.8 HV was perceived in the single pass, third pass and fifth pass FSP.

References

- [1] Chung, D.D.L. Composite Materials Science and Applications, 2nd ed., Springer, New York, 2010
- [2] Abdul Wahab Hashmi, Husain Mehdi, Sipokazi Mabuwa, Velaphi Msomi & Prabhujit Mohapatra, Influence of FSP Parameters on Wear and Microstructural Characterization of Dissimilar TIG Welded Joints with Si-rich Filler Metal. Silicon (2022). <https://doi.org/10.1007/s12633-022-01848-8>
- [3] Abdellah Nait Salah, Sipokazi Mabuwa, Husain Mehdi, Velaphi Msomi, Mohammed Kaddami, Prabhujit Mohapatra, Effect of Multipass FSP on Si-rich TIG Welded Joint of Dissimilar Aluminum Alloys AA8011-H14 and AA5083-H321: EBSD and Microstructural Evolutions. Silicon (2022). <https://doi.org/10.1007/s12633-022-01717-4>.
- [4] Husain Mehdi, R.S. Mishra, Mechanical properties and microstructure studies in Friction Stir Welding (FSW) joints of dissimilar alloy- a review, Journal of Achievements in Materials and Manufacturing Engineering, 77 (1), 31-40, (2016).
- [5] Sampath, P.; Parangodath, V.K.; Udupa, K.R.; Kuruveri, U.B. Fabrication of friction stir processed Al-Ni particulate composite and its impression creep behaviour. Journal of Composites, 2015, 428630, 1-9, <https://doi.org/10.1155/2015/428630>.
- [6] A.Nait Salaha, Husain Mehdi, Arshad Mehmood, Abdul Wahab Hashmid, Chandrabhanu Malla, Ravi Kumar, Optimization of process parameters of friction stir welded joints of dissimilar aluminum alloys AA3003 and AA6061 by RSM, Materials Today: Proceedings, 56 (4), 1675-1684, 2021, <https://doi.org/10.1016/j.matpr.2021.10.288>
- [7] Nicholas, E.D. Developments in the friction stir welding of metals. In Proceedings of the 6th International Conference on Aluminium Alloys,

- Toyohashi, Japan, 5–10 July 1998; 139–151.
- [8] Gupta, M.K. Friction stir process: a green fabrication technique for surface composites—a review paper. *SN Appl. Sci.* 2020, 2, 532, <https://doi.org/10.1007/s42452-020-2330-2>
- [9] Abdul Wahab Hashmi, Husain Mehdi, R. S. Mishra, Prabhujit Mohapatra, Neeraj Kant & Ravi Kumar, Mechanical Properties and Microstructure Evolution of AA6082/SiC Nanocomposite Processed by Multi-Pass FSP. *Transactions of the Indian Institute of Metals*, (2022). <https://doi.org/10.1007/s12666-022-02582-w>.
- [10] Husain Mehdi, R.S. Mishra, Consequence of reinforced SiC particles on microstructural and mechanical properties of AA6061 surface composites by multi-pass FSP, *Journal of Adhesion Science and Technology*, 36(12), 1279-1298, 2022, <https://doi.org/10.1080/01694243.2021.1964846>.
- [11] Husain Mehdi, R.S. Mishra, Effect of multi-pass friction stir processing and SiC nanoparticles on microstructure and mechanical properties of AA6082-T6, *Advances in Industrial and Manufacturing Engineering*, 3, 100062 (2021). <https://doi.org/10.1016/j.aime.2021.100062>
- [12] Husain Mehdi, Arshad Mehmood, Ajay Chinchkar, Abdul Wahab Hashmi, Chandrabhanu Malla, Prabhujit Mohapatra, Optimization of process parameters on the mechanical properties of AA6061/Al2O3 nanocomposites fabricated by multi-pass friction stir processing, *Materials Today: Proceedings*, 56 (4), 1995-2003, 2021, <https://doi.org/10.1016/j.matpr.2021.11.333>.
- [13] Husain Mehdi, R.S. Mishra, Modification of Microstructure and Mechanical Properties of AA6082/ZrB2 Processed by Multipass Friction Stir Processing. *Journal of Materials Engineering and Performance* (2022). <https://doi.org/10.1007/s11665-022-07080-0>
- [14] Liu, G.; Zhang, G.J.; Jiang, F.; Ding, X.D.; Sun, Y.J.; Sun, J.; Ma, E. Nanostructured high-strength molybdenum alloys with unprecedented tensile ductility. *Nat. Mater.* 2013, 12, 344–350.
- [15] Chen, L.Y.; Xu, J.Q.; Choi, H.; Pozuelo, M.; Ma, X.; Bhowmick, S.; Yang, J.-M.; Mathaudhu, S.; Li, X.-C. Processing and properties of magnesium containing a dense uniform dispersion of nanoparticles. *Nature* 2015, 528, 539–543.
- [16] Zhang, W.; Hu, Y.; Zhang, G.; Wang, Z. Formation of nanoscale metallic glassy particle reinforced Al-based composite powders by high-energy milling. *Metals* 2017, 7, 425.
- [17] Huang, G.; Shen, Y.; Guo, R.; Guan, W. Fabrication of tungsten particles reinforced aluminum matrix composites using multi-pass friction stir processing: Evaluation of microstructural, mechanical and electrical behavior. *Mater. Sci. Eng. A* 2016, 674, 504–513.
- [18] Suryanarayana, C.; Al-Aqeeli, N. Mechanically alloyed nanocomposites. *Prog. Mater. Sci.* 2013, 58, 383–502.
- [19] Rajan, H.B.M.; Dinaharan, I.; Ramabalan, S.; Akinlabi, E.T. Influence of friction stir processing on microstructure and properties of AA7075/TiB2 in situ composite. *J. Alloys Compd.* 2016, 657, 250–260.
- [20] Husain Mehdi, R.S. Mishra, Effect of Friction Stir Processing on Mechanical Properties and Wear Resistance of Tungsten Inert Gas Welded Joint of Dissimilar Aluminum Alloys. *Journal of Materials Engineering and Performance* volume, 30, 1926–1937 (2021). <https://doi.org/10.1007/s11665-021-05549-y>
- [21] Jata, K.V., Sankaran, K.K. & Ruschau, J.J. Friction-stir welding effects on microstructure and fatigue of aluminum alloy 7050-T7451. *Metall Mater Trans A* 31, 2181–2192 (2000). <https://doi.org/10.1007/s11661-000-0136-9>.
- [22] Husain Mehdi, R.S. Mishra, Investigation of mechanical properties and heat transfer of welded joint of AA6061 and AA7075 using TIG+FSP welding approach, *Journal of Advanced Joining Processes*, 1, 100003, (2020) <https://doi.org/10.1016/j.jajp.2020.100003>.
- [23] Husain Mehdi, R.S. Mishra, Effect of Friction Stir Processing on Microstructure and Mechanical Properties of TIG Welded Joint of AA6061 and AA7075, *Metallography, Microstructure, and Analysis*, 9, 403–418 (2020). <https://doi.org/10.1007/s13632-020-00640-7>.
- [24] Mishra, R.S.; Ma, Z.Y. Friction stir welding and processing. *Mater. Sci. Eng. R Rep.* 2005, 50, 1–78, <https://doi.org/10.1016/j.mserr.2005.07.001>.
- [25] Jana, S.; Mishra, R.S.; Baumann, J.B.; Grant, G. Effect of stress ratio on the fatigue behavior of a friction stir processed cast Al–Si–Mg alloy. *Scripta Materialia* 2009, 61, 992–995, <https://doi.org/10.1016/j.scriptamat.2009.08.011>.
- [26] Sharma, S.R.; Ma, Z.Y.; Mishra, R.S. Effect of friction stir processing on fatigue behavior of A356 alloy. *Scripta Materialia* 2004, 51, 237–241, <https://doi.org/10.1016/j.scriptamat.2004.04.014>.
- [27] Husain Mehdi, R.S. Mishra, Microstructure and mechanical characterization of tungsten inert gas-welded joint of AA6061 and AA7075 by friction stir processing, *Proceedings of the Institution of Mechanical Engineers, Part L: Journal of Materials: Design and Applications*, 235 (11), 2531-2546 (2021), <https://doi.org/10.1177/14644207211007882>.
- [28] Husain Mehdi, R.S. Mishra, R.S. Analysis of Material Flow and Heat Transfer in Reverse Dual Rotation Friction Stir Welding: A Review, *International Journal of Steel Structures*, 19, 422–434 (2019). <https://doi.org/10.1007/s13296-018-0131-x>.
- [29] Husain Mehdi, R.S. Mishra, Study of the influence of friction stir processing on tungsten inert gas welding of different aluminum alloy. *SN Applied Science*, 1, 712 (2019). <https://doi.org/10.1007/s42452-019-0712-0>.
- [30] Husain Mehdi, R.S. Mishra, Effect of friction stir processing on mechanical properties and heat transfer of TIG welded joint of AA6061 and AA7075, *Defence Technology*, 17 (3), 715-727 (2021). <https://doi.org/10.1016/j.dt.2020.04.014>
- [31] O.T. Middling, L.D. Oosterkamp, J. Bersaas, Friction stir welding aluminium process and applications. *Int. Proc.7 Inter. conf. jt. alum.*, 1998, INALCO98.
- [32] S.S. Mirjavadi, M. Alipour, A.M.S. Hamouda, A. Matin, S. Kord, B.M. Afshari, P.G. Koppad, Effect of multi-pass friction stir processing on the microstructure, mechanical and wear properties of AA5083/ZrO₂ nanocomposites, *J. Alloys Compd.* 726 (2017) 1262–1273.
- [33] V. Ebrahimzadeh, M. Paidar, M.A. Safarkhanian, O.O. Ojo, Orbital friction stir lap welding of AA5456-H321/AA5456-O Al-alloys under varied parameters, *Int. J. Adv. Manuf. Technol.* 96 (2018) 1237–1254.
- [34] H.A. Deore, A. Bhardwaj, A.G. Rao, J. Mishra, V.D. Hiwarkar, Consequence of reinforced SiC particles and post process artificial ageing on microstructure and mechanical properties of friction stir processed AA7075, *Defence Technology* 16 (2020) 1039-1050.
- [35] Husain Mehdi, R.S. Mishra, Influence of Friction Stir Processing on Weld Temperature Distribution and Mechanical Properties of TIG-Welded Joint of AA6061 and AA7075. *Transactions of the Indian Institute of Metals*, 73, 1773–1788 (2020). <https://doi.org/10.1007/s12666-020-01994-w>
- [36] Husain Mehdi, R.S. Mishra, An experimental analysis and optimization of process parameters of AA6061 and AA7075 welded joint by TIG+FSP welding using RSM, *Advances in Materials and Processing Technologies*, 2020, <https://doi.org/10.1080/2374068X.2020.1829952>.
- [37] H. Mohammadzadeh Jamalian, M. Farahani, M. K. Besharati Givi, and M. Aghaei 8 Vafaei (2016), “Study on the effects of friction stir welding process parameters on the microstructure and mechanical properties of 5086-H34 aluminum welded joints,” *International Journal of advanced manufacturing technology*, vol. 83, no. 1–4, pp. 611–621.
- [38] A. Sharma, V.M. Sharma, S. Mewar, S.K. Pal, J. Paul, Friction stir processing of Al6061-SiC-graphite hybrid surface composites, *Mater. Manuf. Process.* 33 (7) (2018) 795–804.
- [39] A.Nait Salah, M. Kaddami, Husain Mehdi, Mechanical Properties And Microstructure Characterization of Friction Stir Welded Joint Of Dissimilar Aluminum Alloy AA2024 And AA7050, *Turkish Journal of Computer and Mathematics Education*, 12(7), 1051-1061 (2021).

Cite this article as: Rohit Kumar, Rakesh Rajpal, Rajesh Kumar, Effect of multipass friction stir processing and reinforcement particles on aluminum alloys of AA7010, *International journal of research in engineering and innovation (IJREI)*, vol 6, issue 4 (2022), 245-251. <https://doi.org/10.36037/IJREI.2022.6406>.